

SCIENTIFIC REPORTS



OPEN

Proton magnetic resonance spectroscopy (^1H -MRS) of the brain in patients with tick-borne encephalitis

Radosław Zawadzki¹, Bożena Kubas², Marcin Hładuński², Olga Zajkowska³, Joanna Zajkowska⁴, Dorota Jurgilewicz², Adam Garkowski¹, Sławomir Pancewicz⁴ & Urszula Łebkowska¹

Tick-borne encephalitis (TBE) is a disease caused by a tick-borne encephalitis virus (TBEV) belonging to the *Flaviviridae* family. The aforementioned virus is transmitted by the bite of infected ticks. In the recent years, TBEV has become a serious public health problem with a steady increase in its incidence, mainly due to the climate changes and spreading the infected ticks into new territories. The standard protocol of TBE diagnosis involves the serological laboratory test with a minor role of imaging techniques such as magnetic resonance imaging. Long-term complications affecting patients daily activities are reported in about 40–50% of the cases. However, no changes are revealed in the laboratory tests or the imaging examination. The development of new imaging techniques such as proton magnetic resonance spectroscopy (^1H -MRS) can broaden the knowledge about TBE, contributing to its prevention. The aim of this study was to assess the usefulness of ^1H -MRS of the brain in patients with TBE. Compared to controls, a statistically significant decrease in the N-acetylaspartate /creatinine ratio was found bilaterally in the right and left thalamus as well as a statistically significant increase in the choline/creatinine ratio in the right and left thalamus.

Tick-borne encephalitis virus (TBEV) poses a serious public health problem, especially, in the endemic areas of Central, Eastern and Northern Europe, in northern China, Mongolia, South Korea and in the Russian Federation. TBEV belongs to the family *Flaviviridae*, genus *Flavivirus*, is transmitted through a tick-bite, or is connected with the consumption of non-pasteurized milk from infected livestock¹. There are three subtypes of the virus causing a human disease: the European subtype, the Far-Eastern subtype and the Siberian subtype² including mainly *Ixodes ricinus* in Europe, *I. persulcatus* predominating in the Siberian subtypes and *I. ovatus* of Far-Eastern TBEV subtype in Japan^{3–5}. The vectors of TBEV are infected ticks. Most cases of TBE occur in the period between April and November with the peak of the tick activity which corresponds with warming of the climate during spring, summer and autumn months and human outdoor activity^{6–8}.

The disease has a biphasic course with an incubation period varying from 2–28 days (usually 7–14 days), and shorter incubation periods after milk-borne exposure with the first phase lasting approximately 1–8 days. In this phase, the patient has nonspecific flu-like symptoms^{9,10}. After about 8 days of remission, in 30–50% of the cases, the second neurological phase begins with symptoms in the form of meningitis (50% of the adult cases), meningoencephalitis (about 40% of the adult patients), myelitis (4–15%)^{11,12}. It is important to note that about 40–50% of the patients who underwent TBE can develop a post-encephalic syndrome which results in permanent CNS function impairment in the form of cognitive disorders and neuropsychiatric complaints^{10,13–15}.

Currently the diagnosis of TBE is based on the laboratory serological tests with a subsidiary role of magnetic resonance (MR) imaging techniques and a minor role of computed tomography (CT) imaging. In the first viral phase of the disease, leukopenia and/or thrombocytopenia can be observed, whilst a mildly elevated number

¹Department of Radiology, Medical University of Białystok, Białystok, Poland. ²Independent Department, Laboratory of Molecular Imaging, Medical University of Białystok, Białystok, Poland. ³Faculty of Applied Informatics and Mathematics, Warsaw University of Life Sciences SGGW, Warsaw, Poland. ⁴Department of Infectious Diseases and Neuroinfections, Medical University of Białystok, Białystok, Poland. Correspondence and requests for materials should be addressed to R.Z. (email: zaw.radoslaw@gmail.com)

Characteristic	No. of Patients (%)
Mean age, years (range)	43.6 (22–64)
Male, sex	15 (60%)
Female, sex	10 (40%)
History of tick bite	9 (36%)
Clinical course of TBE:	
Meningitis	0
Meningoencephalitis*	22 (88%)
Meningoencephalomyelitis*	3 (12%)

Table 1. Epidemiological and clinical characteristics of patients with tick-borne encephalitis. *These patients had consciousness disturbances and/or focal neurological symptoms. Patients with epileptic seizures were not included in the study, because they can change $^1\text{H-MRS}$ results.

of leukocytes in the second encephalic phase¹⁶. The key role in diagnosing TBE plays determination of TBEV specific IgM and IgG serum antibodies obtained by means of a highly specific immunosorbent assay (ELISA), while polymerase chain reaction (PCR) helps in the virus detection only in the first viral phase of the infection. Additionally, the cerebrospinal fluid (CSF) analysis may reveal pleocytosis.

Due to the limited spatial resolution, CT is considered to be less sensitive than MR and has an auxiliary role before the lumbar puncture to exclude brain oedema. To this time there has been a limited number of reports involving macroscopic CNS changes exhibiting hypodense areas in the CNS^{17–19}.

MR imaging can be helpful in diagnosing inflammatory morphological changes in the CNS. The optimal time of the MR scan correlates with the best detectability of the IgM and IgG antibodies in the CSF at around the tenth day of the infection²⁰. A standard MR examination can show lesions in the thalamus, basal ganglia, internal capsule, splenium, cerebellum, peduncles and brainstem, while a small number of patients with encephalomyelodradiculitis, encephalomyelitis, isolated radiculitis, myelodradiculitis had also documented spinal MRI changes^{4,21–34}.

The purpose of this study was to evaluate whether patients with TBE may develop brain metabolite alterations within the brain regions without any macroscopic changes on the conventional MR examination, especially, considering the fact that in about 40–50% of the cases, long-term complications affecting daily activity are reported without any changes in the laboratory test or the imaging examination. It is important to note that to this date and to our knowledge no major studies describing the features of TBE in $^1\text{H-MRS}$ have been conducted in people. We hypothesized that since TBEV infects the brain, it may lead to alterations in the cerebral metabolism measured by $^1\text{H-MRS}$.

Materials and Methods

Study subjects and protocol of proton magnetic resonance spectroscopy. The present study was carried out in 25 patients diagnosed with TBE and 25 healthy controls. Only patients with meningoencephalitis and meningoencephalomyelitis, were included in the study excluding those with meningitis, since they presented no neurological symptoms, thus no $^1\text{H-MRS}$ abnormalities were expected. The clinical course of the disease, age and sex distribution are presented in Table 1. No statistically significant difference was found in age and gender distribution between the two groups. The inclusion criteria were based on the European Centre for Disease Prevention and Control (ECDC) guidelines and consisted of a typical two phase clinical course of TBE, detection of IgM and/or IgG antibodies in blood serum and CSF by ELISA as well as granulocytosis in the CSF examination.

Protocol of MRI and proton magnetic resonance spectroscopy ($^1\text{H-MRS}$). All patients underwent a routine MRI protocol with a single 3.0 Tesla MRI scanner (Biograph mMR, Siemens Healthineers, Erlangen, Germany), using a 16-channel head matrix coil.

Scan was performed between 10th and 14th day of the disease. Routine imaging was carried out prior to spectroscopy to exclude any structural abnormalities and included T1W (TR, 180 ms; TE, 2.5 ms; section thickness, 4.0 mm; intersection gap, 1.0 mm; 27 axial slices; field of view [FOV], 220 × 185 mm; and matrix size, 320 × 320), T2W imaging (TR, 3300 ms; TE, 107 ms; section thickness, 4.0 mm; intersection gap, 1 mm; 30 axial slices; field of view [FOV], 220 × 185 mm; and matrix size, 512 × 512), fluid-attenuated inversion recovery (FLAIR) (TR, 9000 ms; TE, 94 ms; section thickness, 4.0 mm; intersection gap, 1.0 mm; 27 axial slices; field of view [FOV], 240 × 195 mm; and matrix size, 256 × 256), and diffusion weighted images (DWI) (TR, 870 ms; TE, 82 ms; section thickness, 4.0 mm; intersection gap, 1.0 mm; 27 axial slices; FOV 240 × 240 mm; and matrix size 132 × 132; b-value 0, 500, 1000, 1500).

The preparation phase of $^1\text{H-MRS}$ included automatic procedures for water suppression, shimming, and tuning of the radiofrequency and gradient system and an acquisition without water suppression for correction of magnetic field distortions. $^1\text{H-MRS}$ planning was acquired on T1W sequences (TR; 18 ms; TE; 4.97 ms, section thickness 1 mm; intersection gap 0.2 mm; 160 sagittal slices; FOV [230 × 230]; and matrix size 256 × 256) from this sequence, coronal and axial planes were reconstructed with the same technical parameters. $^1\text{H-MRS}$ examinations were performed with the following acquisition parameters: (TR/TE: 2000/135 ms, bandwidth 1200 Hz, number of excitation, 128). A point-resolved spectroscopy sequence (PRESS) was used for the rectangular volume of interest (VOI) selection. Single VOIs were manually located bilaterally within the normal-appearing brain tissue in the basal ganglia, thalami and in the hemispheres of the cerebellum with the size of VOI of 15 × 15 × 15 mm (Fig. 1). VOIs were positioned aiming to cover the regions that had been investigated for the

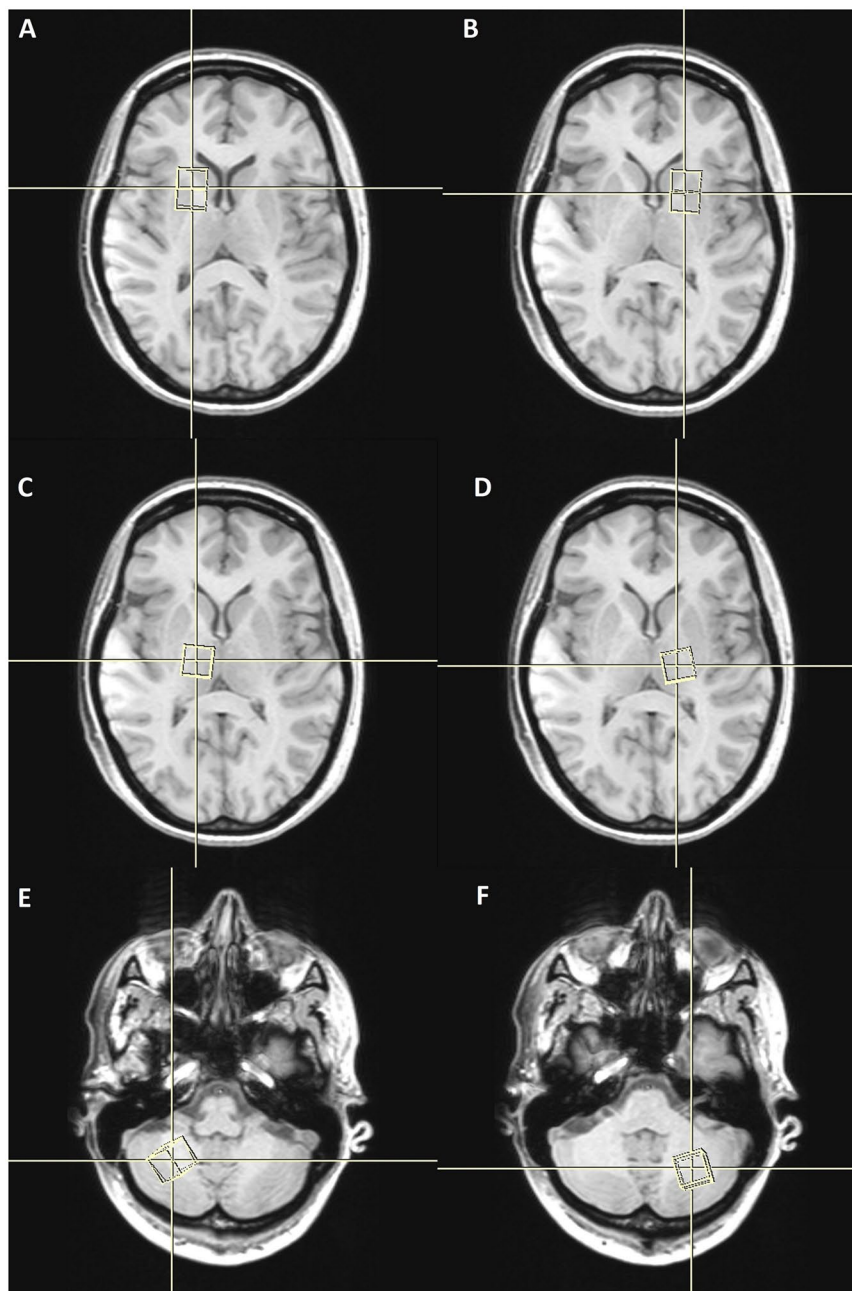


Figure 1. Spatial localization of the VOI in the basal ganglia (A,B), thalami (C,D), hemispheres of cerebellum (E,F).

greatest viral accumulation shown in the previous studies³⁵. The localization of VOIs was confirmed by three orthogonal MR images in the axial, sagittal, and coronal planes. Metabolite ratios were calculated based on the peak integrals of N-acetylaspartate (NAA, 2.01 ppm), creatine (Cr, 3.03), choline-containing compounds, (Cho, 3.23 ppm). The metabolite concentrations (Fig. 2) were analysed using LCmodel (Provencher, 1993) quantification algorithm³⁶.

The MR images were interpreted by a senior MR radiologists (with 20 years of experience in MRI).

Statistical analysis. The significance of differences in the metabolite ratios between TBE and control group were estimated with the unpaired Welch's t test with unequal variances. Since the total of TBE patients and control group is limited, the p-values were bootstrapped for the two tailed t test with 10000 replicates. A value of $p < 0.05$ was considered statistically significant. The robustness of the results was confirmed by means of the nonparametric methods (Kruskal-Wallis test, Wilcoxon rank sum test). The analysis was performed with Stata 15 software.

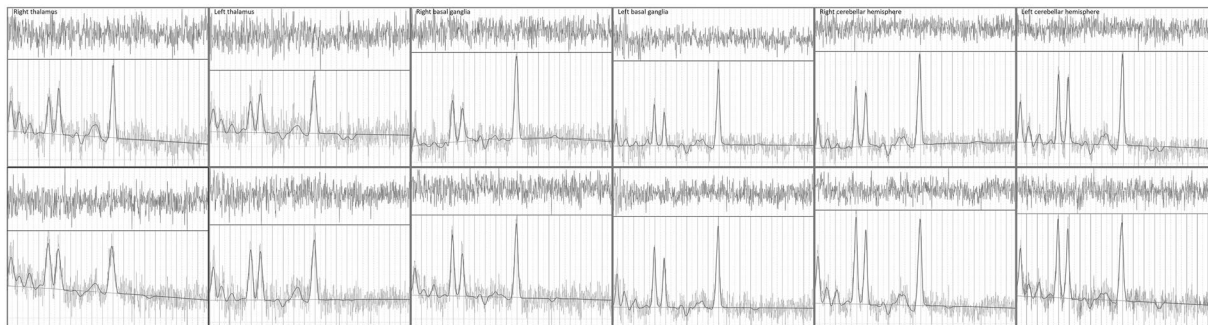


Figure 2. Sample spectra for healthy controls (upper panel) and patients with TBE (lower panel) from the six volumes of interest.

VOI location	NAA/Cr		Cho/Cr	
	Patients	Control group	Patients	Control group
Right thalamus	1,863 ± 0,246*	2,170 ± 0,270	0,358 ± 0,038	0,337 ± 0,062
Left thalamus	1,988 ± 0,365*	2,284 ± 0,234	0,365 ± 0,051*	0,332 ± 0,034
Right basal ganglia	1,389 ± 0,171*	1,631 ± 0,644	0,288 ± 0,044	0,311 ± 0,145
Left basal ganglia	1,441 ± 0,173	1,442 ± 0,207	0,279 ± 0,035	0,273 ± 0,062
Right cerebellar hemisphere	1,563 ± 0,307	1,545 ± 0,196	0,326 ± 0,065	0,311 ± 0,039
Left cerebellar hemisphere	1,577 ± 0,223	1,489 ± 0,220	0,342 ± 0,048*	0,312 ± 0,038

Table 2. 1H-MRS data for patients and control group. * $p < 0.05$.

Ethical approval and informed consent. The study was approved by the ethics committee of the Medical University of Bialystok (approval no. R-I-002/340/2015) and was conducted according to the principles expressed in the Declaration of Helsinki. A written informed consent was obtained from all patients.

Results

The NAA/Cr ratio was significantly lower in the left and right thalamus (bootstrapped $p = 0.000$ and $p = 0.001$, respectively). Additionally, the difference was also found in the right basal ganglia confirmed by both the one-sided t-test and nonparametric methods. A statistically significant increase in the Cho/Cr ratio was observed in the left thalamus and left cerebellar hemisphere (bootstrapped $p = 0.007$ and $p = 0.016$ respectively), as shown in Table 2. There was no statistically significant brain metabolite changes in other study areas.

The examination was performed between 10th and 14th day of the disease. No macroscopic CNS lesions were found in the study group after MRI examination, apart from one patient presenting the dimmed nonspecific lesion observed in the left frontal lobe and bilateral diffused hyperintense lesions in the posterior horns of the lateral ventricles.

Discussion

Findings presented in our study suggest that the TBEV infection may lead to metabolite alterations in the CNS, which can be in turn associated with the generation and persistency of psychiatric symptoms. The metabolite changes in the CNS of patients affected by TBEV could explain their clinical state, and can possibly affect their further loss of life quality. To the best of our knowledge, no $^1\text{H-MRS}$ studies carried out in patients with TBE have been reported. Only one report on the examination performed in veterinary medicine involving dog models has been found³⁷. The authors of that paper showed changes from a mild to moderate decrease in NAA and Cr peaks, and a mild increase in glutamate/glutamine peaks. It is worth mentioning that the TBEV infection is characterised by the distribution of the flavivirus (FV) attachment factors and receptors (GAGs, HSPGs, CD81, claudins, DC-SIGN) promoting FV entry into the neurons, glia and non-CNS tissues, which facilitates FV entry into these cells via a multi-step process, sometimes involving one or more of these attachment factors³⁸. This leads to the rapid microglial/macrophage activation, release of soluble inflammatory mediators and over expression of MHC class I molecules as well as the recruitment of cytotoxic T cell, leading to three possible mechanisms of tissue destruction: by direct neuronal injury, by induction of an inflammatory response inducing the neuronal death, or a combination of these two mechanisms. The study revealed the following principal findings: NAA/Cr levels decreased bilaterally in the thalamus and the right-sided basal ganglia, while Cho/Cr levels increased in the left thalamus and left cerebellar hemisphere^{39,40}. NAA is a marker of neuronal density and integrity, so the decreased values of NAA in the examined area prove that the axonal injury has taken place, even without any macroscopic changes in a routine MR examination both in the thalami and in the basal ganglia. A statistically significant increase in Cho/Cr was observed in the left thalamus and left cerebellar hemisphere. Choline as one of the components of the phospholipid metabolism of the cell membrane. Thus, disturbances in the Cho levels can cause problems with transporting and cell proliferation within the area affected. Moreover, acetylcholine, a

precursor of choline, is a neurotransmitter which plays a major role in expressing emotions, whereas fluctuations in the levels of choline and compounds containing choline can explain emotional disturbances. No correlations were found between the fluctuations of metabolite levels and macroscopic changes in the study group. Only one patient had a subcortical nonspecific dimmed lesion in the left frontal lobe and bilateral diffused hyperintense lesions in the posterior horns of the lateral ventricles. This can prove that metabolite level changes occur first before macroscopic changes can be seen.

Conclusions

The reduction of NAA/Cr and increase Cho/Cr ratio observed in patients that suffered from TBE can suggest a direct neurotropic activity of the TBEV. Our study has proved that ¹H-MRS can be a sensitive tool for assessing brain metabolite changes in patients with TBE.

References

- Kaiser, R. The clinical and epidemiological profile of tick-borne encephalitis in southern Germany 1994–98: a prospective study of 656 patients. *Brain*. **122**, 2067–78 (1999).
- World Health Organization. Vaccines against tick-borne encephalitis: WHO position paper. *Wkly Epidemiol Rec*. **86**, 241–56 (2011).
- Sumilo, D. *et al.* Tick-borne encephalitis in the Baltic States: identifying risk factors in space and time. *Int J Med Microbiol*. **296**, 76–9 (2006).
- Bender, A., Schulte-Altdorneburg, G., Walther, E. U. & Pfister, H. W. Severe tick borne encephalitis with simultaneous brain stem, bithalamic, and spinal cord involvement documented by MRI. *J Neurol Neurosurg Psychiatry*. **76**, 135–7 (2005).
- Walder, G. *et al.* Serological evidence for tick-borne encephalitis, borreliosis, and human granulocytic anaplasmosis in Mongolia. *Int J Med Microbiol*. **296**, 69–75 (2006).
- Mansfield, K. L. *et al.* Tick-borne encephalitis virus - a review of an emerging zoonosis. *J Gen Virol*. **90**, 1781–94 (2009).
- Lindquist, L. & Vapalahti, O. Tick-borne encephalitis. *Lancet*. **371**, 1861–71 (2008).
- Kaiser, R. Tick-borne encephalitis. *Infect Dis Clin North Am*. **22**, 561–75 (2008).
- Bogovic, P. & Strle, F. Tick-borne encephalitis: A review of epidemiology, clinical characteristics, and management. *World J Clin Cases*. **3**, 430–41 (2015).
- Mickiene, A. *et al.* Tickborne encephalitis in an area of high endemicity in lithuania: disease severity and long-term prognosis. *Clin Infect Dis*. **35**, 650–8 (2002).
- Taba, P. *et al.* EAN consensus review on prevention, diagnosis and management of tick-borne encephalitis. *Eur J Neurol*. **24**, 1214–61 (2017).
- Bogovic, P., Lotric-Furlan, S. & Strle, F. What tick-borne encephalitis may look like: clinical signs and symptoms. *Travel Med Infect Dis*. **8**, 246–50 (2010).
- Misić Majerus, L., Daković Rode, O. & Ruzić Sabljčić, E. Post-encephalitic syndrome in patients with tick-borne encephalitis. *Acta Med Croatica*. **63**, 269–278 (2009).
- Tomazic, J. *et al.* The clinical features of tick-borne encephalitis in Slovenia. A study of 492 cases in 1994. *Antibiotika Monitor*. **12**, 115–20 (1996).
- Günther, G., Haglund, M., Lindquist, L., Forsgren, M. & Sköldenberg, B. Tick-borne encephalitis in Sweden in relation to aseptic meningo-encephalitis of other etiology: a prospective study of clinical course and outcome. *J Neurol*. **244**, 230–8 (1997).
- Kaiser, R. Tick-borne encephalitis: Clinical findings and prognosis in adults. *Wien Med Wochenschr*. **162**, 239–243 (2012).
- Horger, M. *et al.* Imaging findings in tick-borne encephalitis with differential diagnostic considerations. *Am J Roentgenol*. **199**, 420–7 (2012).
- Marjelund, S., Tikkakoski, T., Tuisku, S. & Räisänen, S. Magnetic Resonance Imaging Findings and Outcome in Severe Tick-borne Encephalitis. Report of Four Cases and Review of the Literature. *Acta Radiologica*. **45**, 88–94 (2004).
- Waldvogel, K., Bossart, W., Huisman, T., Boltshauser, E. & Nadal, D. Severe tick-borne encephalitis following passive immunization. *Eur J Pediatr*. **155**, 775–779 (1996).
- Holzmann, H. Diagnosis of tick-borne encephalitis. *Vaccine*. **1**, 36–40 (2003).
- Ponfick, M. *et al.* Meningoencephaloradiculomyelitis after tickborne encephalitis virus infection: a case series. *Eur J Neurol*. **19**, 776–782 (2012).
- Stich, O., Reinhard, M. & Rauer, S. MRI scans of cervical cord provide evidence of anterior horn lesion in a patient with tick-borne encephalomyeloradiculitis. *Eur J Neurol*. **14**, 5–6 (2007).
- Cruciatti, B., Beltrame, A., Ruscio, M., Viale, P. & Gigli, G. L. Neurological manifestation of tick-borne encephalitis in north-eastern Italy. *Neurol Sci*. **27**, 122–124 (2006).
- Pfefferkorn, T., Feddersen, B., Schulte-Altdorneburg, G., Linn, J. & Pfister, H. W. Tick-borne encephalitis with polyradiculitis documented by MRI. *Neurology*. **68**, 1232–1233 (2007).
- Enzinger, C., Melisch, B., Reischl, A., Simbrunner, J. & Fazekas, F. Polyradiculitis as a predominant symptom of tickborne encephalitis virus infection. *Arch Neurol*. **66**, 904–905 (2009).
- Valdueza, J. M., Weber, J. R., Harms, L. & Bock, A. Severe tick borne encephalomyelitis after tick bite and passive immunisation. *J Neurol Neurosurg Psychiatry*. **60**, 593–594 (1996).
- Vollmann, H., Hagemann, G., Mentzel, H. J., Witte, O. W. & Redeker, C. Isolated reversible splenic lesion in tick-borne encephalitis: a case report and literature review. *Clin Neurol Neurosurg*. **113**, 430–433 (2011).
- Alkadhi, H. & Kollias, S. S. MRI in tick-borne encephalitis. *Neuroradiology*. **42**, 753–755 (2000).
- Lorenzl, S., Pfister, H. W., Padovan, C. & Yousry, T. MRI abnormalities in tick-borne encephalitis. *Lancet*. **347**, 698–699 (1996).
- Pfister, H. W., Lorenzl, S. & Yousry, T. Neuroradiographic manifestations of encephalitis. *N Engl J Med*. **337**, 1393–1394 (1997).
- Czupryna, P. *et al.* MRI and planimetric CT follow-up study of patients with severe tick-borne encephalitis. *Infect Dis (Lond)*. **48**, 74–81 (2016).
- Von Stulpnagel, C. *et al.* MRI-imaging and clinical findings of eleven children with tick-borne encephalitis and review of the literature. *Eur J Paediatr Neurol*. **20**, 45–52 (2016).
- Racz, A. *et al.* Isolated meningomyeloradiculitis following infection with tick borne encephalitis virus. *Clin Neurol Neurosurg*. **114**, 1263–1265 (2012).
- Marjelund, S., Jaaskelainen, A., Tikkakoski, T., Tuisku, S. & Vapalahti, O. Gadolinium enhancement of cauda equina: a new MR imaging finding in the radiculitic form of tick-borne encephalitis. *Am J Neuroradiol*. **27**, 995–997 (2006).
- Gelpi, E. *et al.* Visualization of Central European tick-borne encephalitis infection in fatal human cases. *J Neuropathol Exp Neurol*. **64**, 506–12 (2005).
- Provencher, S. W. Estimation of metabolite concentrations from localized *in vivo* proton NMR spectra. *Magn Reson Med*. **30**, 672–9 (1993).
- Sievert, C., Richter, H., Beckmann, K., Kircher, P. R. & Carrera, I. Comparison between proton magnetic resonance spectroscopy findings in dogs with tick-borne encephalitis and clinically normal dogs. *Vet Radiol Ultrasound*. **58**, 53–61 (2017).
- Neal, J. W. Flaviviruses are neurotropic, but how do they invade the CNS? *J Infect*. **69**, 203–15 (2014).

39. Stocco, A., Lebiere, C. & Anderson, R. J. Conditional Routing of Information to the Cortex: A Model of the Basal Ganglia's Role in Cognitive Coordination. *Psychol Rev.* **117**, 541–574 (2010).
40. Steriade, M. & Llinás, R. R. The Functional States of the Thalamus and the Associated Neuronal Interplay. *Physiological Reviews.* **68**, 649–742 (1988).

Acknowledgements

This study was funded by the Medical University of Białystok, Poland (grant number: N/ST/ZB/16/003/1127).

Author Contributions

R.Z. and A.G. conceived and led the project. R.Z. developed the theoretical concepts and performed the simulation study. M.H. and D.J. developed the experimental apparatus. B.K. performed the experiments, with assistance from S.P. and U.L. wrote the paper with input from all co-authors. O.Z. and J.Z. discussed the results and revised the manuscript.

Additional Information

Competing Interests: The authors declare no competing interests.

Publisher's note: Springer Nature remains neutral with regard to jurisdictional claims in published maps and institutional affiliations.



Open Access This article is licensed under a Creative Commons Attribution 4.0 International License, which permits use, sharing, adaptation, distribution and reproduction in any medium or format, as long as you give appropriate credit to the original author(s) and the source, provide a link to the Creative Commons license, and indicate if changes were made. The images or other third party material in this article are included in the article's Creative Commons license, unless indicated otherwise in a credit line to the material. If material is not included in the article's Creative Commons license and your intended use is not permitted by statutory regulation or exceeds the permitted use, you will need to obtain permission directly from the copyright holder. To view a copy of this license, visit <http://creativecommons.org/licenses/by/4.0/>.

© The Author(s) 2019